Fall 2022

Wireless Coupled Feed Structure for Additively Manufactured Conformal Antennas

Blake Roberts
Embry-Riddle Aeronautical University, roberb25@my.erau.edu

Wireless Coupled Feed Structure for Additively Manufactured Conformal Antennas

By

Blake Roberts

A Thesis Submitted to the Faculty of Embry-Riddle Aeronautical University in Partial Fulfillment of the Requirements for the Degree of Master of Science in Electrical and Computer Engineering

12/2022

Embry-Riddle Aeronautical University

Daytona Beach, Florida

Wireless Coupled Feed Structure for Additively Manufactured Conformal Antennas

by

Blake Roberts

This thesis was prepared under the direction of the candidate's thesis committee chairman, Eduardo Rojas, Department of Electrical Engineering and Computer Science, and has been approved by the members of the thesis committee. It was submitted to the Department of Electrical Engineering and Computer Science and was accepted in partial fulfillment of the requirements for the degree of Masters of Electrical and Computer Engineering.

THESIS COMMITTEE:

_____
Committee Chairman
Eduardo Rojas, Ph.D.

_____
Committee Member
Brian Butka, Ph.D.

_____
Committee Member
Jianhua Liu, Ph.D.

_____
Department Chair, Electrical Engineering and Computer Science
Radu Babiceanu, Ph.D.

_____
Associate Vice President for Academics
Christopher Grant, Ph.D.

Acknowledgements

I would like to thank the staff, faculty, and fellow students at Embry-Riddle for enabling me to grow and learn while at the university. My fellow students within the WideLab were instrumental in my success over the years. Countless times you all have taken time out of your research to help me learn about a new topic or trouble shoot a design or measurement.

I particularly want to thank the professors of The Department of Electrical Engineering and Computer Science for supplying me with the knowledge and skill necessary to get to this point in my academic career. Specifically, I would like to thank the members of my committee, Dr. Butka, Dr. Liu, and Dr. Rojas, for their long-standing commitment to my education as phenomenal professors for many of my classes as well as their time spent reviewing and giving guidance for this thesis. Dr. Butka was my first professor at Embry-Riddle and from the first day of classes has always been the type of professor to encourage the most out of students and has been instrumental in my growth as a student and an engineer. Dr. Liu has always been an extremely patient professor who has always taken the time to make sure I had wrapped my head around some of the more complicated topics. Finally, a thank you to my committee chair, Dr. Rojas, who has been the strongest guiding force in my academic career. With his depth of knowledge, extreme drive, and optimistic encouragement, I have been able to do and achieve more than I ever imagined I could.

Abstract

Due to advancements in additive manufacturing, it is possible to create electromagnetic devices that can be conformally printed directly onto 3D surfaces using conductive inks and dielectric pastes. Instance, the traditional antenna radomes that had the purpose of protecting the antenna on its inside can now become the antenna itself. With the components on the surface of the structure, instead of inside if it, a direct feed line would require cutting through dielectric layers and creating a direct electrical connection, also called vertical interconnect access (VIA). Such interconnects are frequent sources of failures, especially in applications that are subject to vibrations, high accelerations, and extreme changes in temperature. This thesis presents the study of a feed structure that can couple electromagnetic energy between two layers, that is compatible with well-known additive manufacturing technologies, radiofrequency enabling energy transfer without the need of VIAs. The proposed wireless feed structure has been optimized for maximum bandwidth and lowest insertion loss over the bandwidth of interest. The presented wireless feed design can be generalized to common non-flat RF components. In this work a solution is suggested using a transition from microstrip line to microstrip line that is generalized enough to fit into most design needs. The feed design is demonstrated on a planar form using the traditional 4003C Roger's laminate achieving a 27% bandwidth, with a center frequency of 7 GHz, and the minimum insertion loss of -1.84 dB. An additive manufacturing prototype is made with the nScrypt additive manufacturing system using ABS and CB028 conductive ink. The results are then compared to the use of a VIA to show the viability of the wireless feed structure for additively manufactured antennas.

Table of contents

List of Tables & Figures

Abbreviations

ABS - Acrylonitrile butadiene styrene

AFRL - Air force research lab

DoD - Department of Defense

dB - Decibels

FDM - fused deposition modeling

GHz - Gigahertz

MSM Feed- microstrip/slotline/microstrip feed

PEEK - Polyether ether ketone

USAF - United States Air Force

UV - Ultraviolet

VNA - Vector Network Analyzer

RF - Radio Frequency

Symbols

Z_{sl} - Impedance of the slot line

Z_{ms} - Impedance of a microstrip

λ - Wavelength in free space

λ' - Wavelength of the feed line

n - Coupling ratio

ε_r - Relative permittivity

Wm - Width of microstrip feedline

Ws - Width of slotline at the center

Ws2 - Width of the slotline at the center of the bowtie design

Ls - Length of slotline

d - Thickness of each dielectric layer

Chapter I: Introduction

Researchers and officers of the United States Air Force (USAF) identify additive manufacturing (AM) as a necessity for the department of defense (DoD) to invest resources into to allow for more agile and flexible manufacturing needs [1]. This identifies a need to be able to design printable antenna feed structures that can be easily printed, removing the need for post processing. Many defense applications of AM parts required survival under high-stress, vibration, accelerations, and temperatures; hence teams within the U.S. DoD are studying different AM processes to survive harsh environments [2]. In the case of a high stress environment there is a concern of shearing the vertical interconnect accesses (VIAs) or more likely their connections to the printed ink. When compared to bulk copper, conductive inks can be more brittle and electrical connections made with them can become a failure point under stress.

In AM, layers are typically laid out one after another. This means a design that can easily be manufactured in discrete conductive and dielectric layers naturally fits into the manufacturing process. Different conductive layers can be connected using VIAs, however, such VIA structure requires a form of post processing, and they are well known points of failure in high shock environments. In this thesis the idea of a wireless feed structure is studied for its use in 3D printed radio frequency circuits, and as a feed structure for antennas.

The parts of the study are: (a) a review of relevant theorical background and related electromagnetic coupling structures in the literature; (b) generation of a generalized solution for a wireless feed and its optimization using electromagnetic numerical simulations; (c) a design, manufacturing, and testing of a wireless feed prototype using both conventional methods and AM.

The criteria of success are to: (a) maintain a usable bandwidth of 20-25% such that the feed structure can be used to feed an antenna; (b) minimize losses, to make sure the structure is not

detrimental to the overall network, ideally less than 1 dB of insertion loss; and (c) achieve a structure that is compatible with AM processes.

The content in this thesis is distributed according to the following. Chapter I presents an introduction to an identified problem and propose criteria for the solution: Chapter II describes research done into this field and draws upon the literature for inspiration for a design: Chapter III goes into detail about the proposed solution, its refinements, and simulations of the proposed structure: Chapter IV details the manufacturing and testing of the prototype design: Chapter V details the manufacturing and testing of the 3D printed design: Chapter VI explores a possible improvement to the bandwidth of the structure: Finally Chapter VII summarizes the findings, as well as suggests future developments to the design.

Chapter II: Theoretical Background on Coupling Structures and Literature Review on Additive Manufacturing of RF Packaging

2.1 Wireless Fed Patch Antennas

The concept of a wireless antenna feed is inspired by the traditional patch antenna feed using a microstrip line and a coupling window. In that feed structure a microstrip line is used with a slot cut in the ground plane to couple to a patch antenna, as seen in Figure 2.1. Seeing as this is a popular, yet application specific, form of a wireless feed, it serves as a starting point for the work presented in this thesis. The feed in Fig. 2.1 works by having an aperture in the ground plane of a microstrip line in order to let the electromagnetic fields extend past the ground plane and are directed into the patch above. A further look into the working of this process was embarked on with the goal to generalize the concept to a geometry that can be applied as a general feed structure.

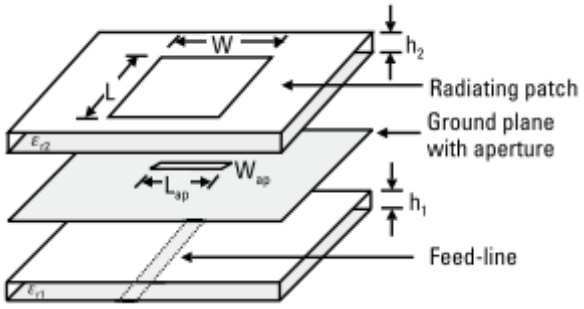

Figure 2.1 a wireless fed patch antenna [3].

2.2 Discussion of Fields Around Microstrip and Slotline

To understand the microstrip-based wireless feed concept better it can be broken down into two common transmission lines, the microstrip line and the slot line. As seen in Figure 2.2, the fields of a microstrip and a slotline are perpendicular to each other. This means if they are

geometrically set 90 degrees to one another the fields will align and cause coupling. With this information a search into structure that use this method was investigated.

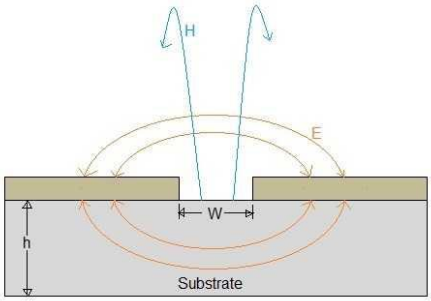

Figure 2.2a slotline fields diagram [4]

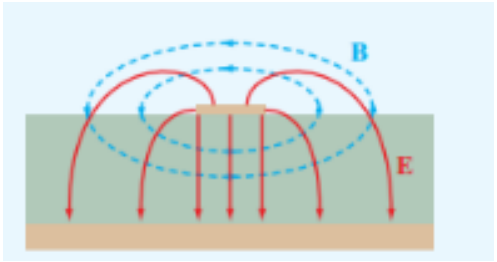

Figure 2.2b microstrip field diagram [5]

2.3 Knor Balun (slotline transition)

A structure was discovered that was designed by Knor that operates as a slotline to microstrip transition [6]. The transition is achieved by cutting a slotline into the ground plane of a microstrip stub. The stub extends past the slot a quarter wave, as seen in Figure 2.3a. 2.3b shows the equivalent circuit for what has been described as the Knor Balun. The impedance transformer ratio of the coupling structure can be calculated with equations 2.1 through 2.5,

$$n=cos(2\pi\frac{D}{\lambda}u\text{-}cot(q_0')sin(2\pi\frac{D}{\lambda}u) \qquad \textit{Eq. 2.1[6]}$$

$$q_0'=2\pi\frac{D}{\lambda}u+tan^{-1}\frac{u}{v} \qquad \textit{Eq. 2.2[6]}$$

$$u=\left[\varepsilon_r-\left(\frac{\lambda}{\lambda'}\right)^2\right]^{\frac{1}{2}} \qquad \textit{Eq. 2.3[6]}$$

$$v=\left[\left(\frac{\lambda}{\lambda'}\right)^2-1\right]^{\frac{1}{2}} \qquad \textit{Eq. 2.4[6]}$$

$$Z_{sl}=\frac{Z_{ms}}{n^2} \qquad \textit{Eq. 2.5[6]}$$

where n is the coupling ratio, Z_{sl} is the impedance of the slot line, Z_{ms} is the impedance of the microstrip section, λ is the wavelength in free space, and λ' is the wavelength in the material. The

traditional microstrip-to-slotline transition is always done by cutting a slot in the ground plane of the existing feed structure and not coupling two separate transmission lines together. However, a structure that achieves coupling between two microstrip lines through a slot is not studied in [6].

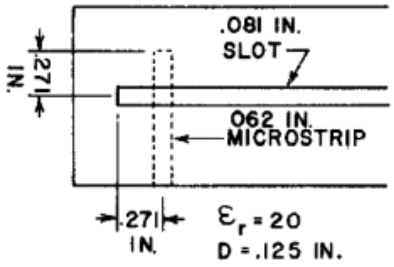

Figure 2.3a microstrip slotline transition [6]

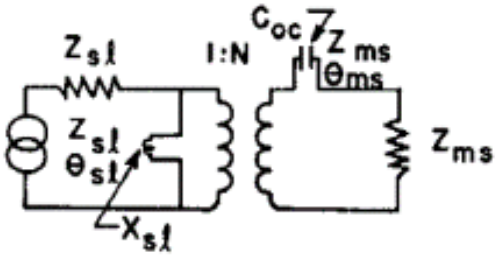

Figure 2.3b equivalent circuit for microstrip slotline transition [6]

2.4 Coupled Line Filter

The suggested geometry comprising of transitions between microstrip and slotline geometries will act in a similar fashion to a coupled line filter, where the input and output are wirelessly connected via an internal coupling structure as shown in Figure 2.4. The main research question is: what will this coupling structure look like and how can it be modeled? Taking inspiration from the Knor transition, the hypothesis is that knowing it is possible to couple from a microstrip to a slot line, we can then couple back efficiently from the slotline to a microstrip geometry to achieve a microstrip-to-microstrip transition. This will produce a microstrip line that is wirelessly coupled to the other with completely discrete layers. There is an expectation that it will act similarly to a coupled line filter, which will limit bandwidth. Such microstrip-microstrip fee structure is presented in Chapter III.

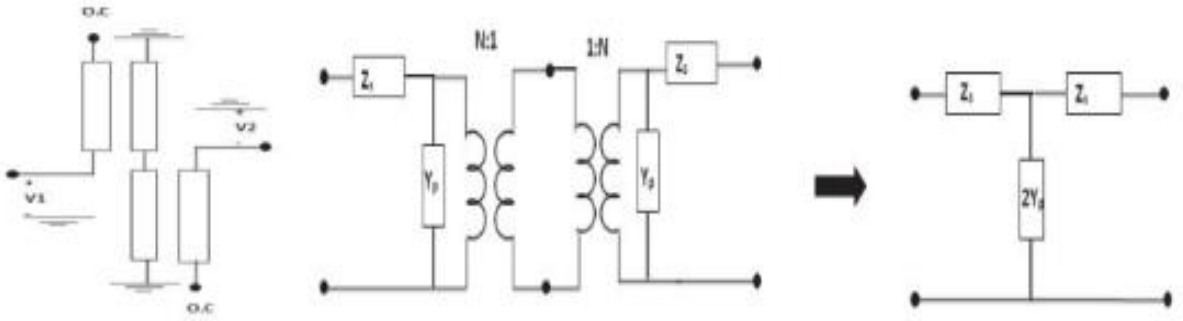

Figure 2.4 coupled line filter and equivalent circuits [7]

2.5 Additive Manufacturing

There is a growing interest in AM antennas and other RF circuits [8][11][13][14]. This is partially due to the fact AM allows for shapes and structures not easily achievable through other methods [14]. A benefit to the additive manufacturing process is that multi-layer boards can be easily manufactured as the process lays material down layer by layer [9]. AM is ideal for rapid prototyping but is also growing and becoming suitable for low volume production as technology advances [11]. As technology advances, the need for interconnecting layers using AM vertical interconnects (VIAs), Figure 2.5a shows said structure under a scanning electron microscope (SEM). It can be seen in Figure 2.5b that as frequency increases the insertion loss begins to increase as well. The insertion loss around the target frequency of this thesis seems to be approximately 1 dB. Additionally, a small air pocket can be seen in the SEM image (Figure 2.5a). While this solution is simple it offers a point of failure for designs that require multilayer interconnects for AM RF circuit

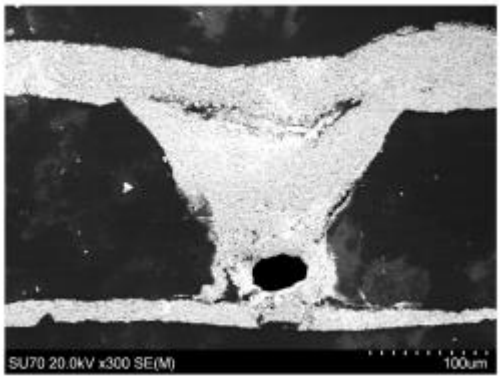

Figure 2.5a electron microscope image of an AM VIA [8]

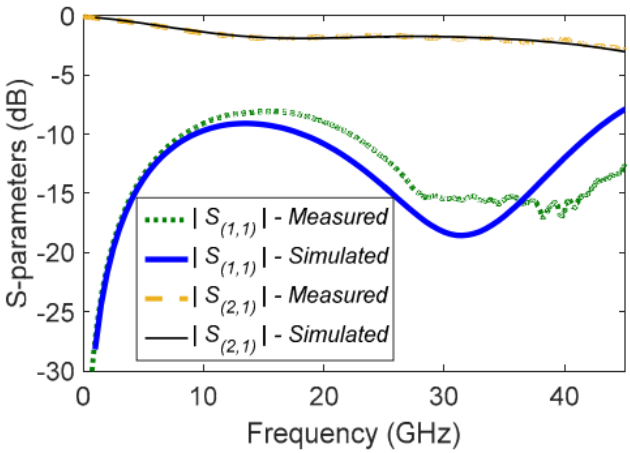

Figure 2.5b insertion and return loss for AM VIA [8]

There are numerous techniques for additive manufacturing that utilize different materials and mediums [10]-[12]. The two main areas of focus in this paper will be fused deposition modeling (FDM) and microdispensing. FDM manufacturing is a process in which extruded thermal plastic is laid down line by line creating discrete layers of plastic. Microdispensing is a manufacturing method that uses a positive pressure pump to extrude a liquid or paste through a control value allowing for dispensing volume control of hundreds of picoliters [10].

Chapter III: Design and Simulations of a Broadband Wireless Feed

3.1 Design & Simulation

As seen in Chapter II, both slot line and microstrip have fields that are not contained within the structure of the geometry. The hypothesis is that this behavior can be leveraged to couple between the two microstrip transmission lines and force an excitation through coupling alone. Such coupling can be seen in Knor's microstrip to slot line transition described in Chapter II as well as the microstrip antenna fed through coupling [6][3]. By orienting the microstrip perpendicular to the slot line the magnetic fields align between the two transmission lines. However, in Knor's design the coupling slot is placed on the ground plane of the microstrip line. The wireless feed design process starts with Knor's geometry, and modifications to it such that it is a constructed as a stack of 3 separate transmission line conductive layers, i.e., microstrip, slotline, and back to microstrip (MSM). This MSM transition will allow for transmission of radio frequency waves without the need to have a direct electrical connection between the layers. Starting with the Knor's microstrip to slotline transition, with a target frequency of approximately 7 GHz and an input impedance of 50 ohms, a design is created. Using equation 2.1-2.5, it can be calculated that the slotline impedance should be 60 ohms.

Based on equation 3.1 the wavelength of the slot can be computed as 28.4 mm for the Rogers 4003C commercial RF laminate for a center frequency of 7 GHz

$$\frac{\lambda_s}{\lambda_0} = \sqrt{\frac{2}{\varepsilon_r+1}} \qquad \text{Eq. 3.1 [16]}$$

However, since the slotline is a non-TEM waveguide the impedance cannot be uniquely defined [16][17]. Moreover, the assumptions made in attempts to create a close formed expression assume high permittivity while the materials used here are much lower permittivity [16]. Using a material with high permittivity would contain the fields inside the substrate likely reducing the

effectiveness of the coupling structure. Based on empirical data shown by Janaswamy and Schaubert, an approximation of slot impedance vs. slot width is shown in Figure 3.1[18]. As permittivity is reduced the required width to reach the desired value of 60 ohms becomes increasingly small and hard to achieve.

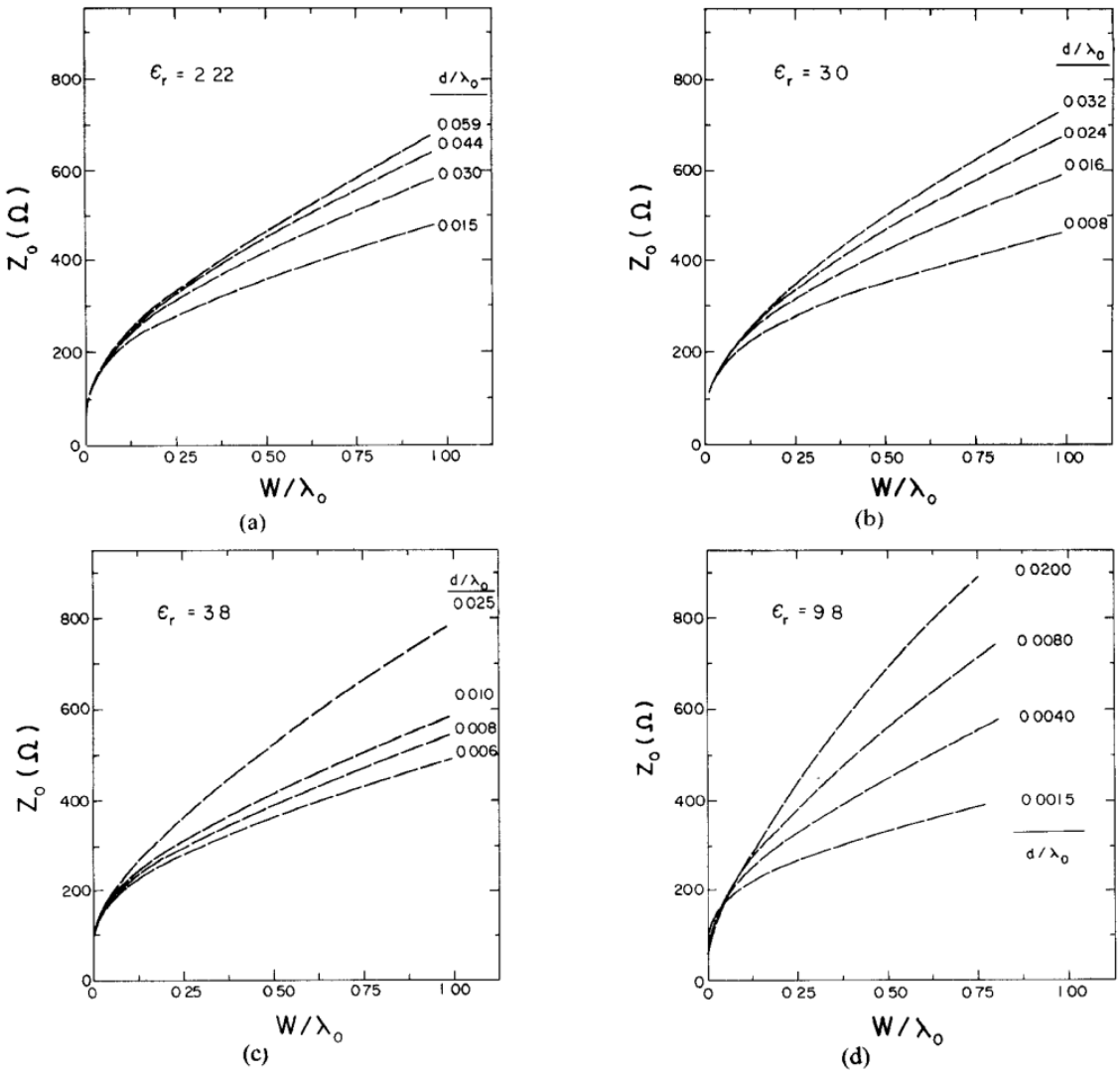

Figure 3.1 empirically determined impedance of slotline [18]

With the knowledge that these models do not perfectly match a real slotline's behavior, nor a slotline that is coupling to two microstrip, it was decided to obtain this value empirically by

sweeping the value of the width of the slot line, in simulation. Thus, tuning the impedance to best match the structure within the limitations.

Before the MSM transition is implemented in a printed design a prototype using conventional methods is designed to act as a proof of concept. Using sapproximations in this section a design gemoetry shown in Figure 3.2 is used as a baseline for the optimizations, the dimentions used can be seen in Table 3.1. The material for the prototype design was chosen to be Rogers 4003c for the initial prototype due to its low loss, and ease to manufacture on which system?

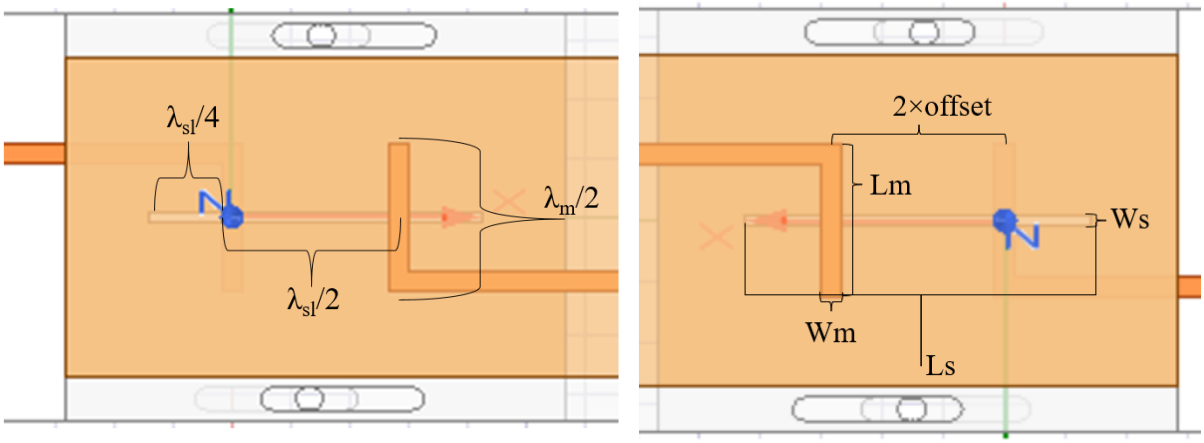

Figure 3.2 original design concept for the MSM transition.

Variable	Value	Description
Offset	7.1 mm	Distance from the center of the slot to the center of the feed stub
Ls	28.4 mm	Length of slot
Ws	0.9 mm	Width of slot
Wm	1.7 mm	Width of microstrip feed stub
Lm	12.7 mm	Length of the microstrip feed stub
d	0.75 mm	Thickness of each dielectric layer

Table 3.1 values used for Baseline MSM design

To model and simulate the design Ansys HFSS was used. The initial design was created based on the calculations above, and an initial simulation was run using a frequency sweep of 5.5 GHz to 10 GHz. Figure 3.3 shows the initial 3d model created.

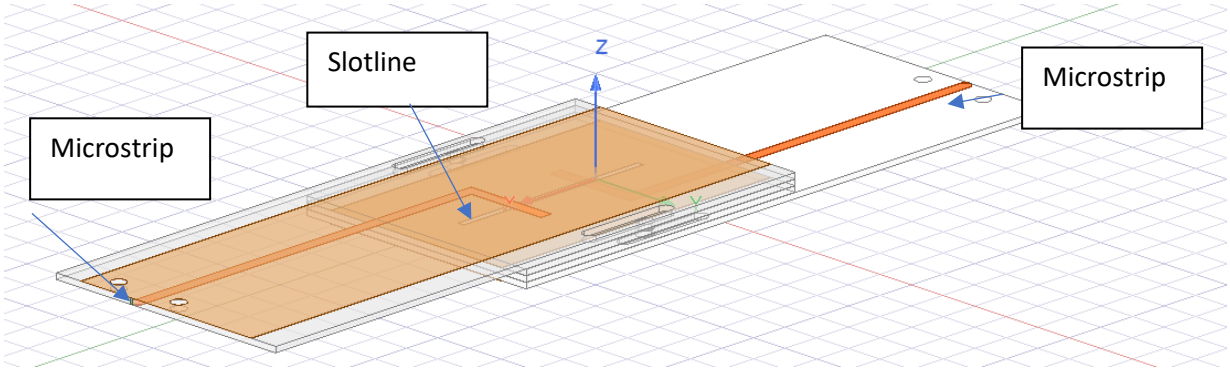

Figure 3.3 3D model of the MSM feed structure

3.2 Electromagnetic Simulation Results of the MSM Prototype

The geometry shown in Figure 3.2 is modeled in Ansys High-Frequency Structure Simulator (HFSS) version 2021 R2. The response of the transmission from the microstrip line port on the left to the microstrip output port on the right (Figure 3.3) can be seen in Figure 3.4a. The dielectric is defined with a relative electric permittivity of 3.5, and a loss tangent of 0.0027[23].

The geometry has the dimensions listed in Table 3.1. The width of the slotline was swept from 0.1 mm to 1.5 mm and it was found that the optimal width was found to be 0.9 mm. The peak was also found to be a bit low at about 6 GHz with a value of -1.35 dB. The simulated 3 dB bandwidth is about 10% from the S-parameter response plotted in Figure 3.4. The simulated response shows that the concept of the MSM feed structure can efficiently couple energy between the microstrip lines. However, further optimization of the geometry is described in Section 3.3 and 3.4 to achieve better bandwidth and insertion loss.

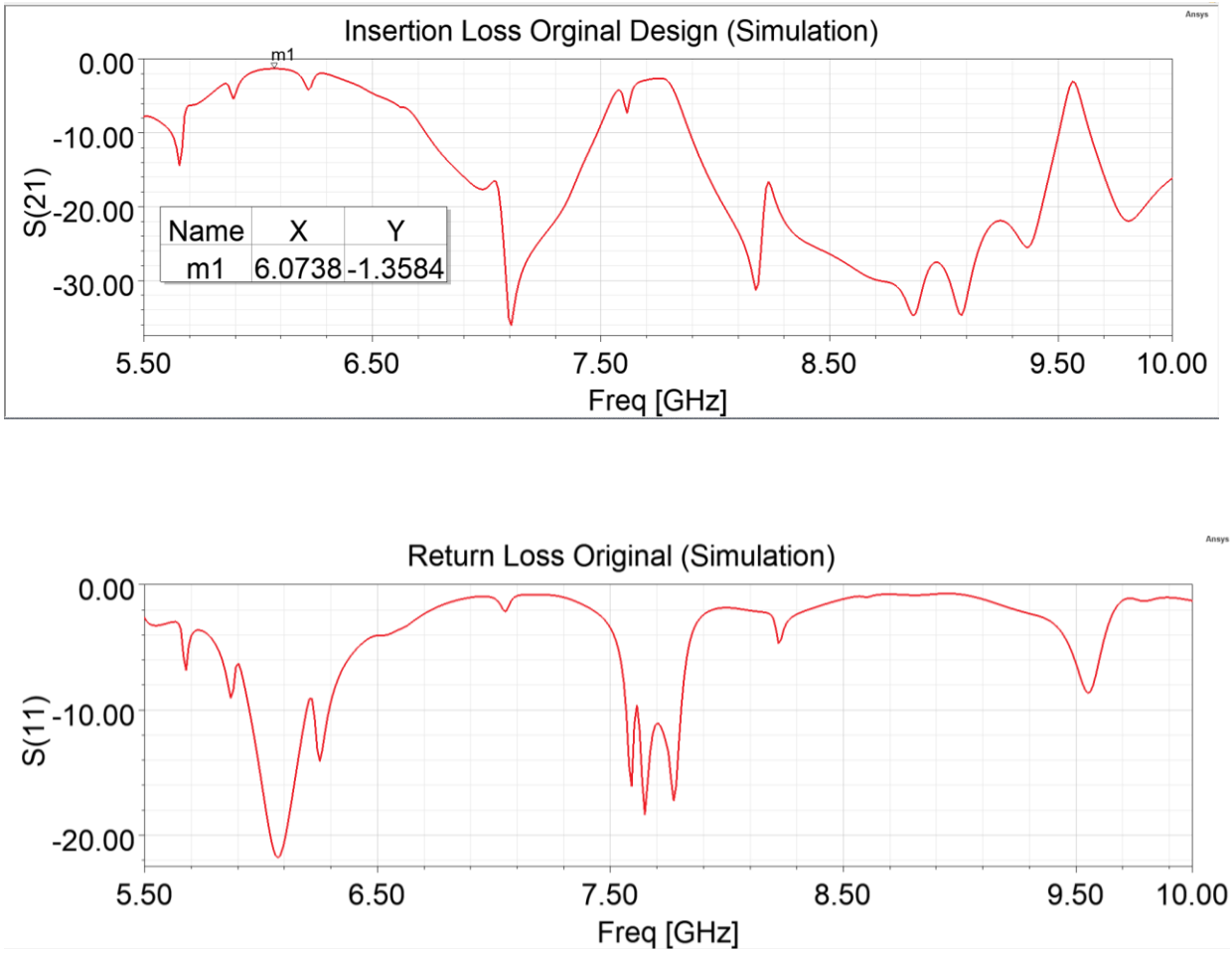

Figure 3.4 (a)S(2,1) and S(1,1) (b) simulation of the original design of the MSM geometry as shown in Figure 3.2.

3.3 Discussion of Simulation Results & Tuning of the Structure

Simulations show that the geometry from Figure 3.4 can couple power between the two microstrip lines. However, the bandwidth can be improved. To increase coupling the idea to shift the microstrip feedline in half a wavelength was attempted, meaning the offset value is changed from 7.1 mm to -7.1 mm. The idea being to increase the amount of surface area of the lines interacting with the slot line in the middle. It is clear looking at the field distribution shown in Figure 3.5 that the electric fields were overall stronger on the slot line leading to the use of this design moving forward with tuning.

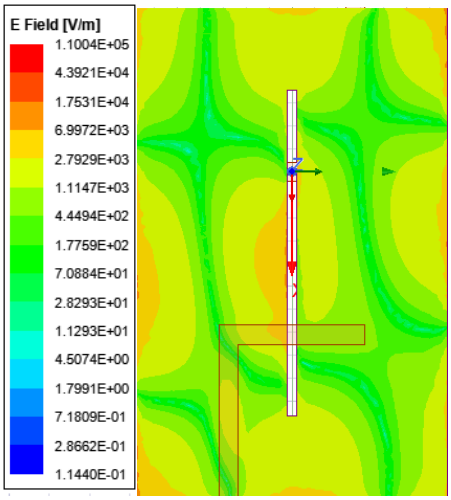

Figure 3.5a electric field of original structure

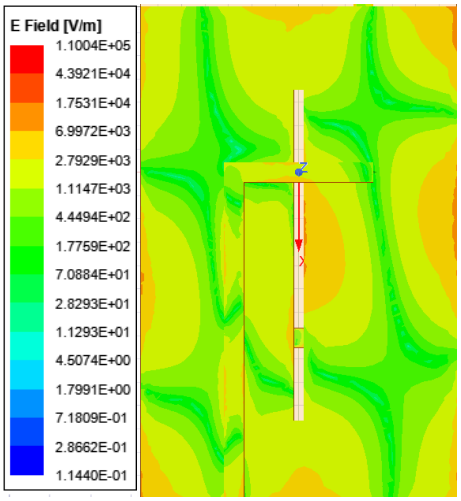

Figure 3.5b electric field of staggered feed structure

Another issue with the design is the overall length of the structure. Even if the feed lines are shortened it still would measure approximately 42.6 mm, i.e. the ideal theoretical length for the slotline is 1.5 x λ_s. One way to minimize the length of the overall design is to experiment with shortening the slotline below a full wavelength. One wavelength slotline length was chosen based on the Knor balun design [6]. However, Kumar and Ray state that the length of the length of the

slotline for a coupled patch antenna is typically a half wavelength [3]. This was explored by shorting the slot to one half wavelength of the slot line wavelength as seen in section 3.4.

The frequency response shown in Figure 3.4 has a center frequency that is lower than the target frequency of 7 GHz, which suggests that the overall dimensions, respect to the wavelengths, can be reduced to adjust for this frequency shift. A design shift is considered that uses an effective permittivity given in equation 3.2

$$\frac{\lambda_{st}}{\lambda_0} = \sqrt{\frac{1}{\varepsilon_r}} \qquad \text{Eq. 3.2}$$

The wavelength calculations for the slotline assume a structure with air on top and dielectric underneath [16]. However, it is believed that this structure will have a wavelength similar to strip line as it is a conductor sandwiched between the same dielectric. Based on the results obtain on the initial geometry simulation, the assumptions for the wavelength for the slotline has been adjusted to 22.9 mm and the results are shown in Section 3.4.

3.4 Wireless Feed Design with Enhanced Slotline and Microstrip Dimensions

Using the three major changes discussed in the previous section and after gemetrical optimizations sweeps of Lm and Ls variables, a a design with an enhanced bandwidth and reduced is chosen and shown in Figure 3.6. The slotline length is set to 12 mm, with the distance between the microstrip stubs being 6 mm. This is close to the quarter wavelength of the stripline at the target frequency of 7 GHz. The design criteria in a generlized form is a 50 ohm line as for a microstrip as an input. The stubs are are slightly shoreter than one half wavelength in length and centered about the slot. The distance between each stub is one half the length of the slot, which was approximately one wavelenth of stripline in length. The width of the slot was an optimized parameter that was determined to be 0.9 mm for this design but will likely have to be adjusted in

simulation using optimizing tools for a general design. Figure 3.6 shows the 3D model of the enhanced design of the structure.

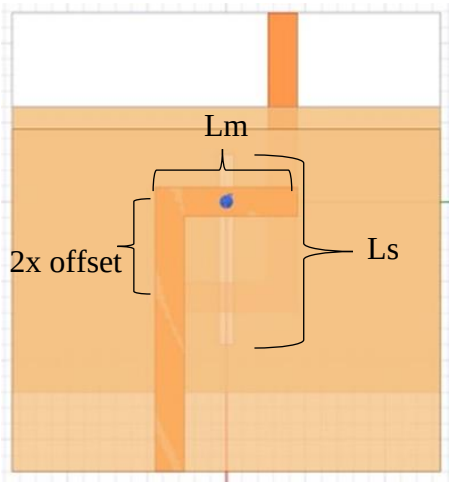

Figure 3.6a general geometry of the enhanced coupling structure

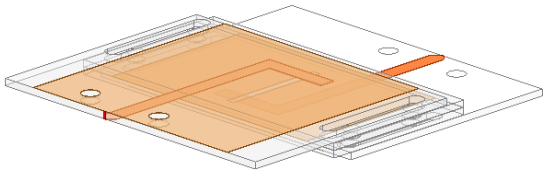

Figure 3.6b isometric view of enhanced coupling structure

Variable	Value	Description
Offset	-6 mm	Distance from the center of the slot to the center of the feed stub
Ls	12 mm	Length of slot
Ws	0.9 mm	Width of slot
Wm	1.8 mm	Width of microstrip feed stub
Lm	8.9mm	Length of the microstrip feed stub
d	0.75 mm	Thickness of each dielectric layer

Table 3.2 values used for Enhanced MSM design

Based on electromagnetic simulations of different combinations of the geometrical parameters for Ls and Lm as well, as some minor adjustments to Wm and Lm for impedance matching, it is determined that a separation of a λ/4 offers maximum coupling between the two

microstrip lines shown in Figure 3.7. Figure 3.7 also shows that with a 90-degree change in phase the observed fields the peak travels the length of the offset, showing the stubs are one quarter wave apart.

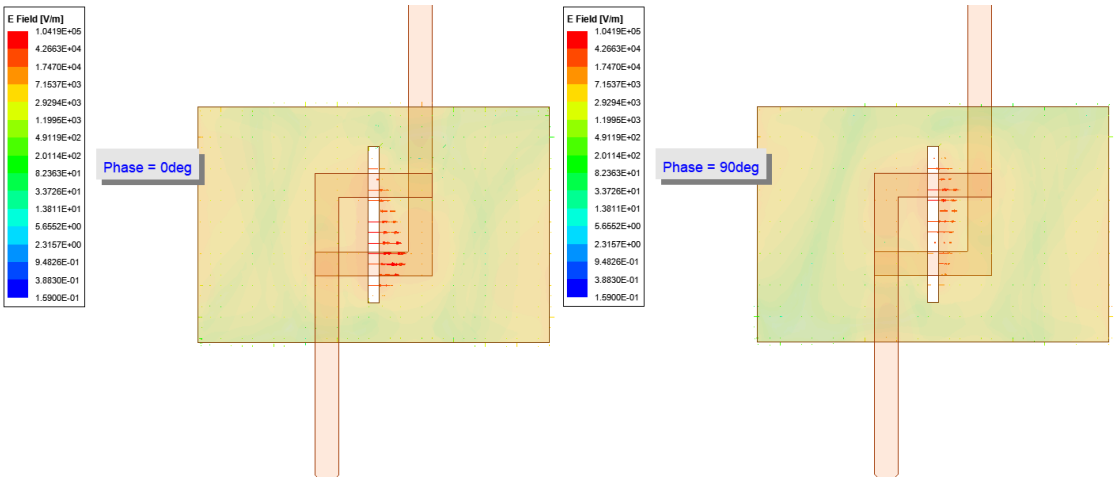

Figure 3.7 fields showing quarter wave separation of stubs

3.5 Comparison Between the Baseline Design and Enhanced Design

The simulated response for the baseline design as seen in Figure 3.9 shows a minimum insertion loss of 1.35 dB at 6.07 GHz but the bandwidth was far below the target value of 1.4 GHz. Additionally, the physical size is 42.6 mm in length, not counting the extended microstrip feed lines. The enhanced design shown in Figure 3.8 is two thirds the size for the slot section with a similar insertion loss of 1.03 dB at 7.00 GHz and a return loss of 25.09 dB at 7.04 GHz. The bandwidth has increased considerably on the enhanced design when compared with the baseline, as seen in Figure 3.10, achieving a 25% fractional bandwidth. The enhanced design is selected for prototype manufacturing.

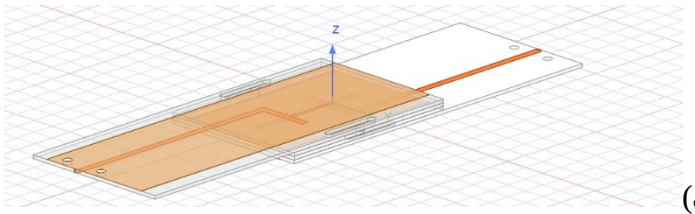

(a)

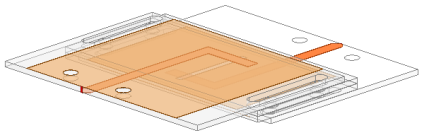

(b)

Figure 3.8 geometries of the wireless feed geometry for (a) the baseline design, and (b) the design with enhanced response

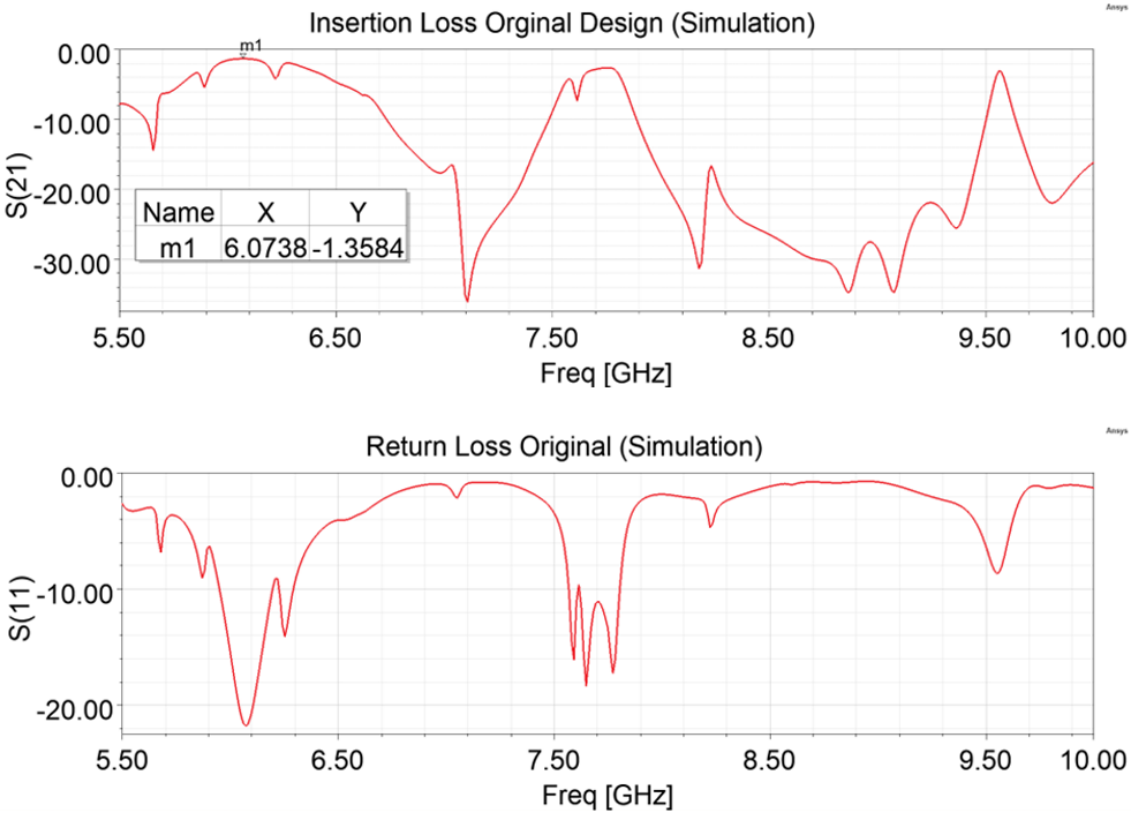

Figure 3.9 baseline design Insertion and return loss

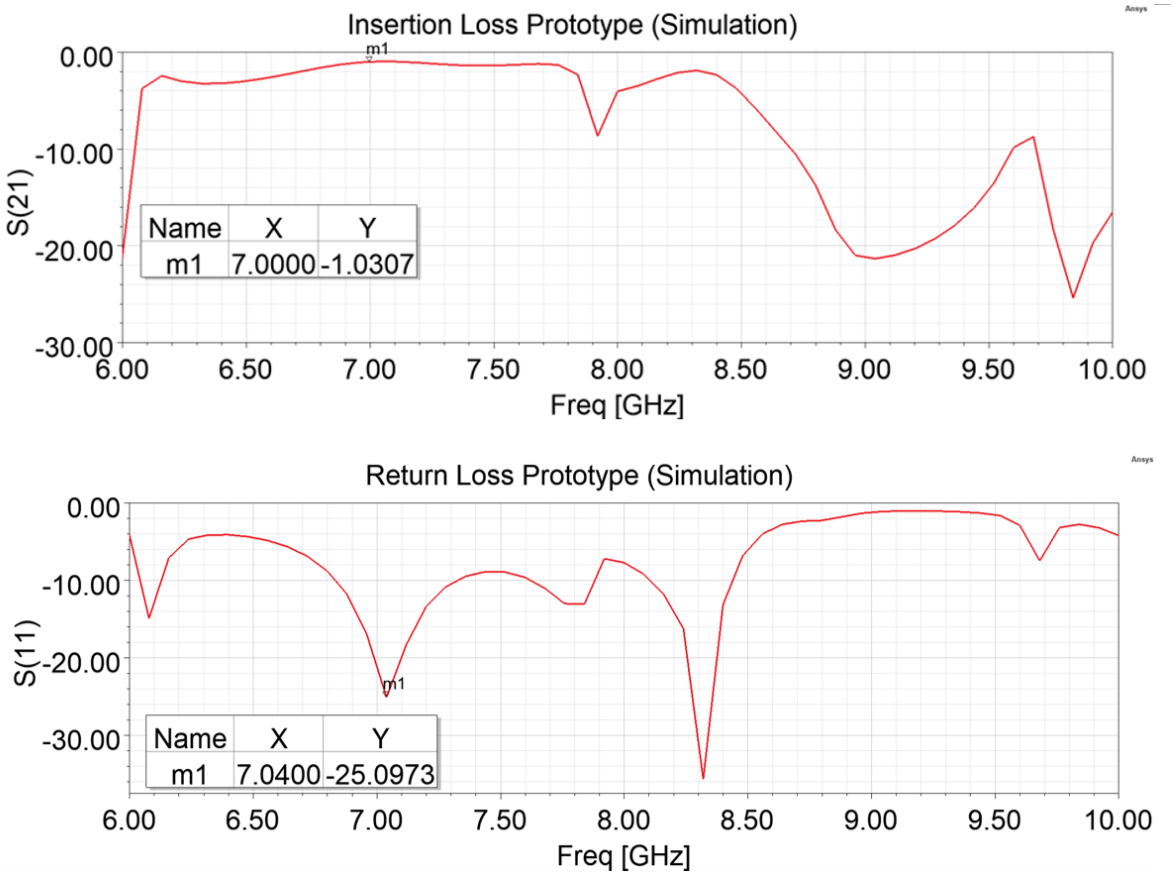

Figure 3.10 insertion loss of the enhanced wireless feed geometry

Chapter IV: Experimental Results of the Wireless Feed Prototypes

4.1 Manufacturing

The LPKF U4 Protolaser laser mill, Figure 4.1a, is used to manufacture the boards for the prototype design. The mill operates by running a hash pattern over the material that it will cut out using a picosecond laser with a wavelength of 355 nm. Then another tool path is used to heat the strips of metal with the laser, melting the adhesive and delaminating the copper from the board. This process is much faster and requires less power than ablating all the copper off the board with the laser for the selected substrate and machine. The hash process steps require tuning of the parameters using the maximum power of 4.8 W and 2 passes, to successfully remove the copper layer. Furthermore, if the hash parameters are not properly set, it is also possible to over-etch the substrate causing changes in the effective electric permittivity of the transmission line. Additionally, if the heat toolpath is overdone the board itself can overheat, also changing its electrical properties. It was noted in the first set of boards produced had a rough texture and the performance of the feed structure was significantly degraded to the point of being nonfunctioning due to the over-milling of the boards. It can be seen in Figure 4.1a that the board is slightly grey, despite the material usually being bright white. This greying was still observed for the minimal power setting for copper removal for the Rogers 4003C board. The laser machining parameter for successful copper removal are kept constant over the entire experiment for consistency, and minimal over-etching and over-heating of the material effects on permittivity were observed for the manufactured samples.

End-launch coaxial to microstrip connectors are attached to the manufactured boards as shown in Figure 4.1b, solder is applied to the connector pin to ensure proper connection to the

microstrip line. The structure is assembled in its sandwich-like structure by using the precut holes on the Rogers substrate, to screw it together with Teflon screws (Figure 4.1b).

Figure 4.1a LPKF U4 Protolaser

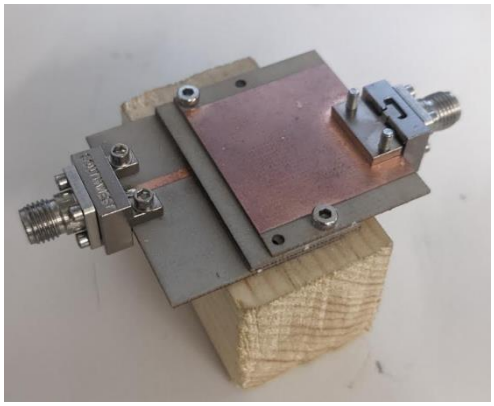

Figure 4.1b MSM Rogers 4003C Prototype

4.2 Wireless Feed Prototype S-Parameters Measurement

A Keysight E5071C ENA is used to measure the S-parameters of the MSM transition. The calibration was preformed using the Keysight N4433A Ecal device, with the machine set to a sweep from 6 to 10 GHz with 801 points. Due to the design of the feed having a ground plane on each end it is reasonable to assume most of the fields will be contained in the structure and

therefore the nearby objects should not have much impact, if any, on the measurement itself. Figure 4.2 shows a comparison between the simulated and measured S(2,1) responses.

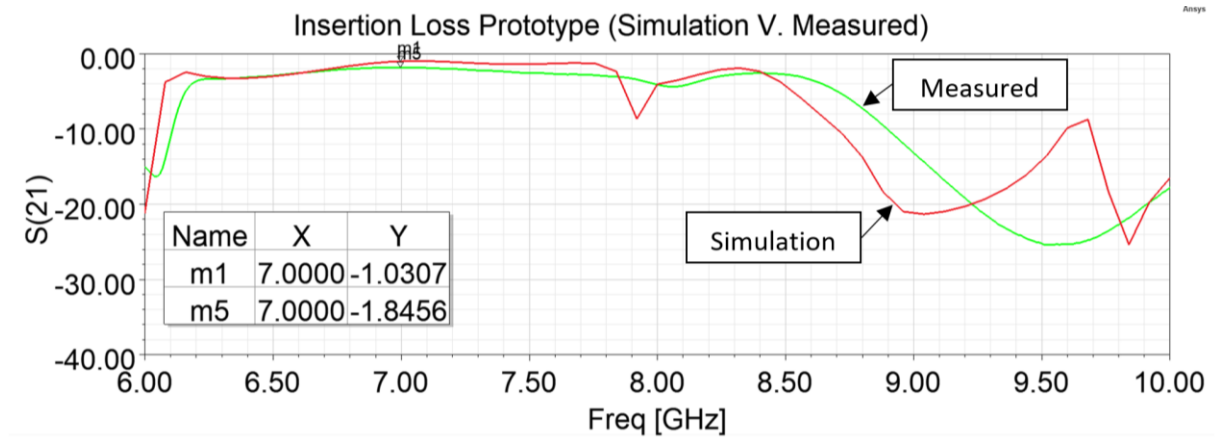

Figure 4.2 insertion loss of prototype simulation verses measured

4.3 Analysis of Results of the Manufactured MSM Structure

The simulated and manufactured designs closely align with one another, with a minimum insertion loss of 1.03 dB and -1.84 dB, for the simulated and measured responses, respectively. The measured 3-dB-bandwidth is slightly higher than the simulation by 25%, for a measured fractional bandwidth of 27%. A frequency up-shift of 0.1 GHz on the lower cut-off frequency is observed on the manufactured samples with respect to the simulations. Response frequency shifts can be associated with variations on the material properties by the manufactured, as well as effects of the laser machining and geometrical deviations. The increase of loss can be associated with unaccounted additional conductor and radiation losses. The results in Figure 4.3 verify the effectiveness of the MSM structure and serve as a base for the design and manufacturing of an AM version of the structure.

Chapter V: Additive Manufacturing of the Wireless Feed

5.1 Manufacturing Equipment and Process

For ease of manufacturing the substrate material that was used for the printing version of the design was ABS. The design will have added loss because of the lossiness of abs due to a loss tangent between 0.005 and 0.019 with most sources placing it near 0.007[19]-[22]. Acrylonitrile butadiene styrene (ABS) is used due to its popular use in AM as well as its ease of manufacturing [8]. CB028 is used as the conductive ink for printing the traces, which typically show an effective electric RF conductivity of around 2 MS/m [12], is easily printable, and is a common ink chosen for 3D printed RF circuits [8][10]-[16].

The manufacturing took place using nScrypt (Figure 5.1) to first print the ABS layer using the FDM print head with a 100-micron nozzle. The nozzle temperature was set to 240 C and the bed to 100 C. Once the ABS part was printed a layer of CB028 was printed on top and cured using the heated bed. This was repeated for each section until the full design was complete.

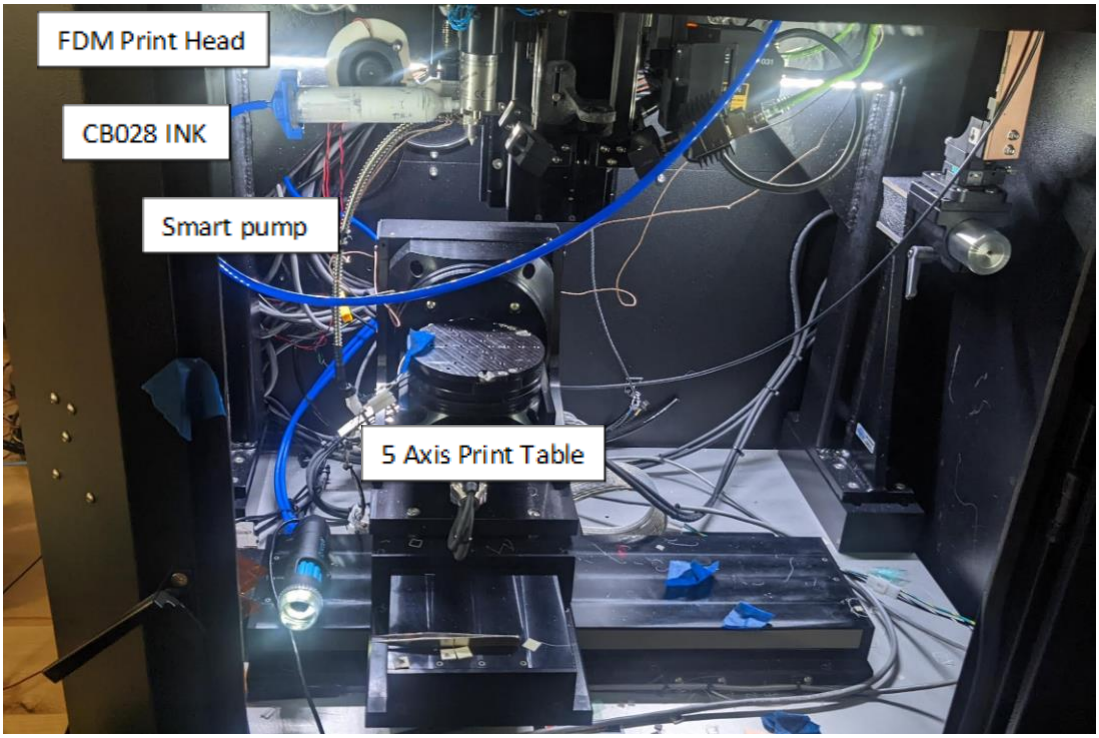

Figure 5.1 NScrypt tabletop machine used to print the final design

5.2 Results

The Keysight VNA was set up and calibrated similar to section 4.2, with a sweep from 6 GHz to 12 GHz and 401 points. The printed sample (Figure 5.3b) was then measured with the results shown in Figure 5.2. The center frequency was measured to be at 8.85 GHz with an insertion loss of 5.1328 dB.

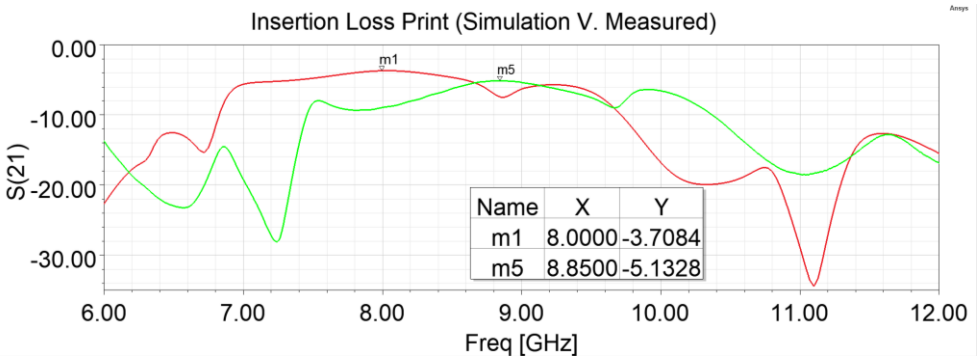

Figure 5.2 printed vs Simulated ABS design insertion loss

5.3 Discussion of Results

From the simulation and the measurements of the printed design. It is evident that there is a degradation in perforce as compared to the commercial laminate prototype. The 3-dB-bandwidth of the simulation is 23.5% and the one for the AM sample is 13.6%. The drop in bandwidth for the AM sample is due to the pronounced ripple in the pass band prematurely dropping the insertions loss below -3 dB from the peak value. The frequency shift shown between the measured and simulated data is most likely accounted for by a change in permittivity, as well as deviations in Lm and Ls. The increased loss compared to the prototype designs comes from the lossiness of ABS, especially compared to Rogers 4003C with a loss tangent anywhere from two times to six time higher [19]-[23].

There is a frequency shift of 0.85 GHz on the center frequency on the response shown in Figure 5.1 that can be associated to the difference of permittivity of ABS from the expected nominal value and potentially material density lower than 100%. ABS can have a wide range of permittivity from 2 to 3.5 [19]-[22] that may change based on manufacturer and printing settings. Although the AM MSM transition shows deviations from the simulations, it verifies the structure can be 3D printed, with room for design improvements to adjust for permittivity and geometrical deviations in the simulations.

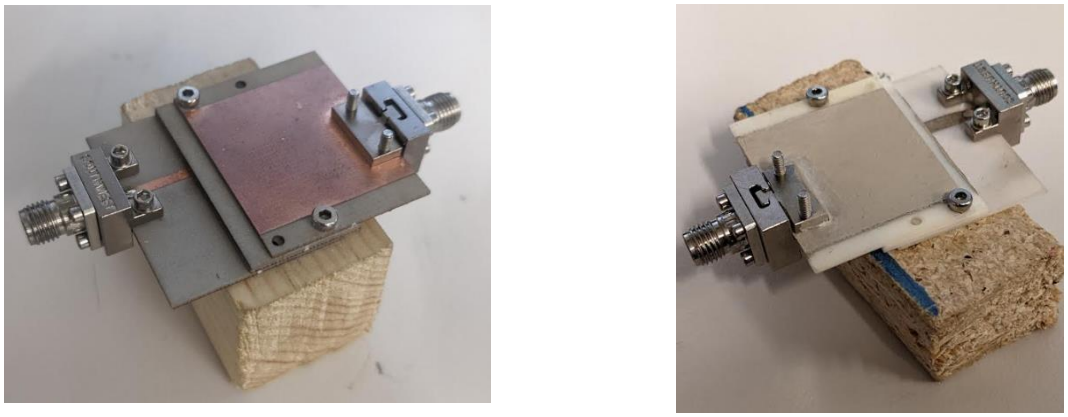

Figure 5.3 (a) milled prototype (b) printed design

Chapter VI: Broadband Wireless Feed

The target application of wireless feeding antenna systems with the MSM structure can benefit from wider bandwidths in the S-parameters response. There are two aspects to creating a better matching network in terms of wideband performance: (a) the bandwidth of the slot structure, and (b) the bandwidth of the microstrip feeding stub, as labeled in Figure 6.1. Both aspects could be a limiting factor of the bandwidth of the feed.

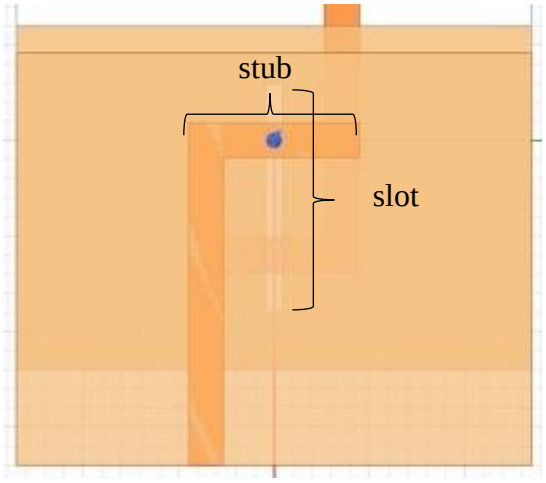

Figure 6.1 highlighting of the stub and slot sections of the MSM feed structure

6.1 Broadband Slotline

Kumar and Ray discuss the design of a wide band aperture coupled patch antenna, similar to that discussed in section 2. They explore multiple different shapes of slot for their design but conclude that a bowtie design as shown in Figure 6.2 is ideal [3]. They however do not offer any design criteria for said bowtie design, seeming to calculate the shape empirically, simply maintaining the minimum width as the original slot width and preserving the original slot length. The maximum width is left to be explored.

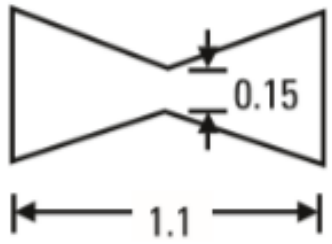

Figure 6.2 bowtie slot design [3]

6.2 Broadband Microstrip Stub

Radial stubs have been used for wide band impedance matching of microstrip line [24]. In an attempt to make a wider range of matched impedance for the microstrip feed structure in Figure 6.3, the idea is to add a radial stub to each side of the feed stub of the microstrip section. This is expected to provide the matching stub while providing an even feed structure on either side of the slot.

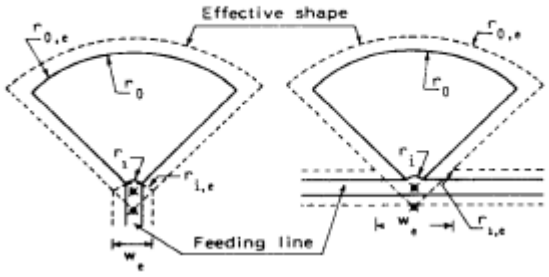

Figure 6.3 radial stub used for matching in microstrip networks [24]

6.3 Design and Simulation Results for the Wideband MSM Transition

The goal is to create a wideband design by combining the wide band radial stub for microstrip and the wide band bowtie for the slot line. A cloverleaf was added to each end of the

microstrip stub to have a balanced feed structure and the slot was converted to the bowtie design shown in Figure 6.4. Using the parameter sweep function in HFSS The values of the radial and bowtie were adjusted, and the most favorable design was selected. The value for Ws2 4 mm and an α value of 40 degrees.

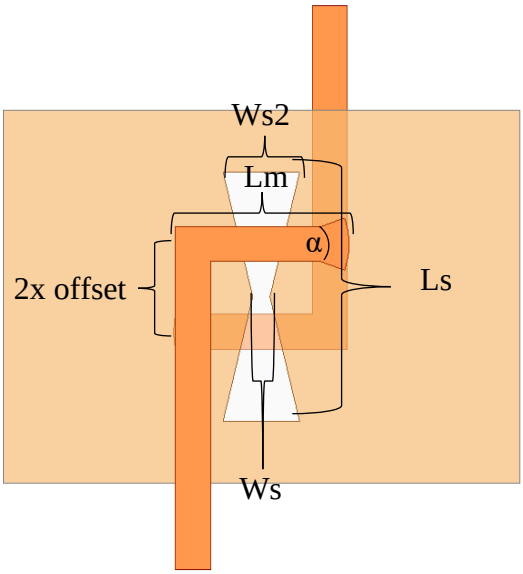

Figure 6.4 wideband adaptation of prototype

Variable	Value	Description
Offset	-6 mm	Distance from the center of the slot to the center of the feed stub
Ls	12 mm	Length of slot
Ws	0.9 mm	Width of slot at center
Ws2	4 mm	Width of slot at ends
Wm	1.8 mm	Width of microstrip feed stub
Lm	8.9mm	Length of the microstrip feed stub
α	40 degrees	Angle of matching stub
d	0.75 mm	Thickness of each dielectric layer

Table 6.1 values used for MSM wideband design

6.4 Simulated Response of the Wideband MSM Structure

The angle of the stub was determined to perform best at 40 degrees, with it having only a minimal performance enhancement to the MSM network when compared to the one with straight stubs shown in Figure 6.5. The biggest factor in the wideband performance of the MSM structure is the addition of the bowtie shaped slot. Although the overall 3-dB-bandwidth of the enhanced MSM structure (Figure 6.4) did not increase when compared with one from Figure 3.6, the flatness of the intersection and return loss responses is greatly improved as seen in Figure 6.5. This design would be interesting to explore further with a more systematic way of creating the structure.

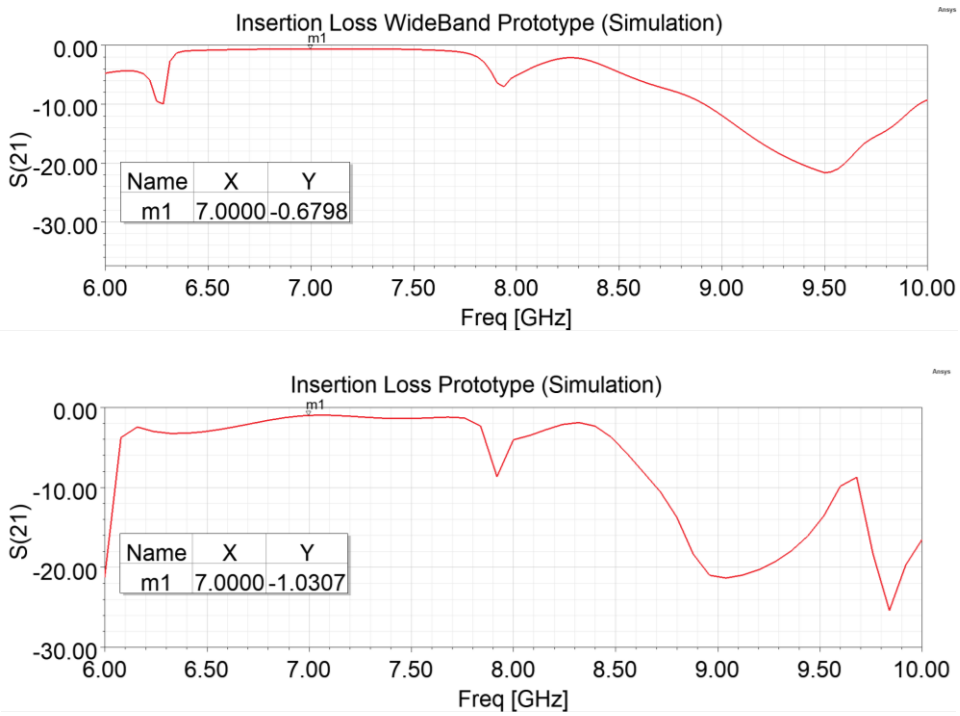

Figure 6.5 insertion loss of simulated wideband prototype vs simulated prototype

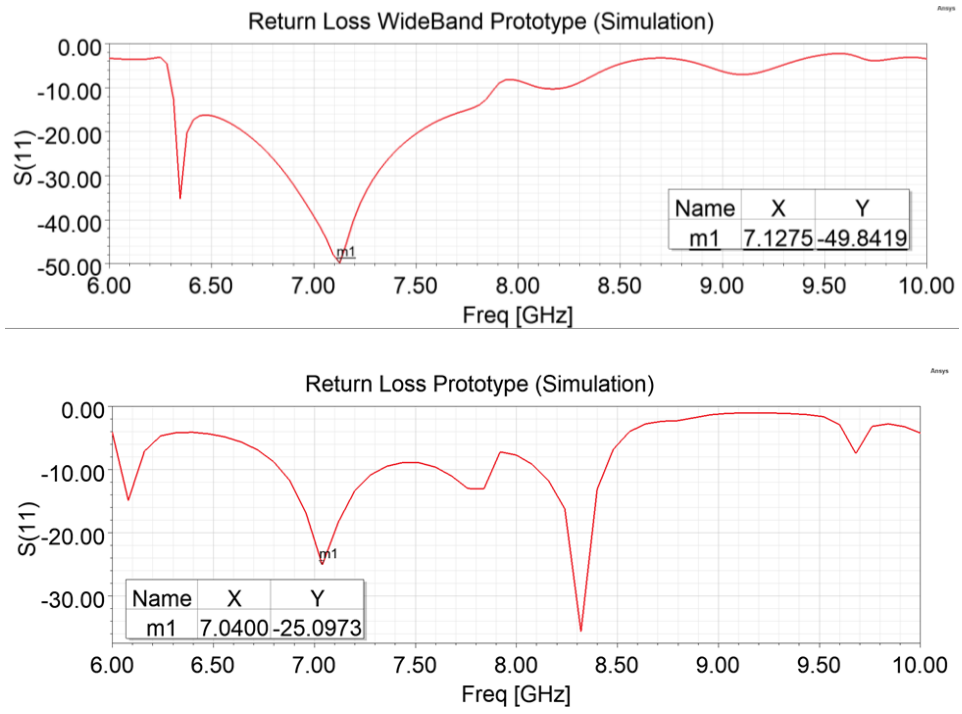

Figure 6.6 return loss of simulated wideband prototype vs simulated prototype

Chapter VII: Conclusion

7.1 Summary

A wireless feed structure to transition from a microstrip geometry (MSM transition) to another microstrip is presented. The design requires four layers of dielectric and five layers of conductor; essentially a slot line stacked between two microstrip lines with ninety-degree half wavelength stubs placed over the slot, one quarter wavelength apart. For the basis of the design equations for strip line are used for wavelength calculation. The width of the slot was tuned using electromagnetic simulations. For the best performance it was found that the feed stubs should be slightly under half a wavelength and the length of the slot should be slightly over half a wavelength. A prototype using traditional manufacturing technique and commercial substrates, as well as another prototype using AM, are fabricated, and tested, confirming the effectiveness of the MSM structure.

7.2 Effectiveness of the MSM transition

Overall, the goal of creating a generalized coupling structure to feed through discrete layers of a printed radio frequency circuit is achieved. It is shown that the MSM geometry design can be created with separate layers and seamlessly integrated into a standard fifty-ohm characteristic impedance system.

It is clear, the structure is sensitive to dielectric losses, which may suggest a better overall performance can be achieved by using lower-loss FDM-compatible dielectrics. In future studies the use of a material such as PEEK or Rogers's radix would lead to an insertion loss closer to the prototype, and therefore a printed structure with much less losses [25]. However, the printed

structure does show the process for manufacturing the wireless feed is viable, with the correct selection of materials.

This design is attempting to replace a more traditional VIA type design when such a design is not practical. While there is the expectation that the structure will have more loss than a direct connection, a simulation is performed to show the performance of a structure using a simple VIA as seen in Figure 7.1. The results of the simulation of this feed are shown in Figure 7.2 for Rogers 4003c and in 7.3 for an ABS substrate. It is clear that there is less loss for an idealized direct feed structure and that the coupled feed is a slight trade off in performance to get the benefits it provides. It can also be seen that even for the VIA structure the ABS and CB028 ink are significantly more lossy than the version using copper and 4003c.

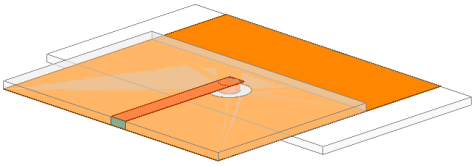

Figure 7.1 feed structure with VIA

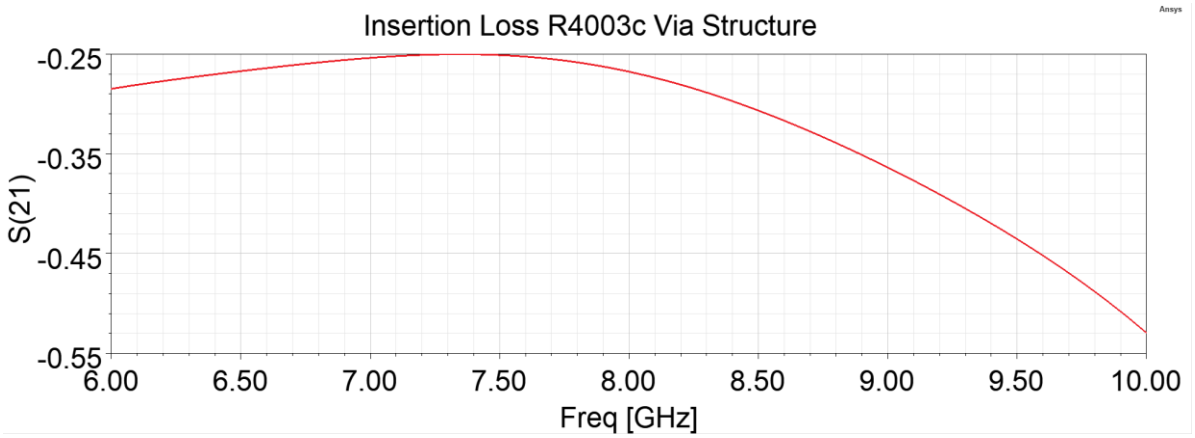

Figure 7.2 insertion loss for microstrip feed structure with VIA on Rogers 4003c

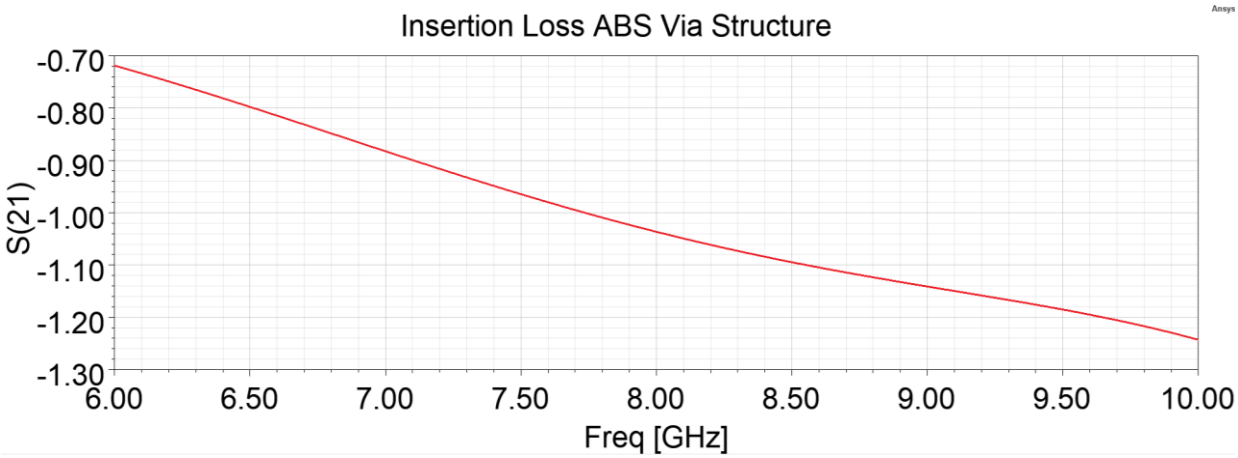

Figure 7.3 insertion loss for microstrip feed structure with VIA on am ABS substrate.

7.3 Future study

One of the limits of the current manufacturing method is that the MSM transition was printed as two separate microstrip lines and another separate slotline. Ideally, these could all be printed as one continuous print without needing to assemble the structure after the fact. This would allow for a seamless transition between the layers of a printed circuit without any need for post processing. While streamlining production it would effectively be the exact same structure and was not in the scope of this design as being able to disassemble the feed for inspection and variations was more important. The manufacturing process could be optimized to make the process much simpler as well as removing variations from the designed performance.

One alternative has been identified but was not able to be obtained in time to manufacture with. Rogers Radix is a low loss UV resin that can be manufactured on a DLP or SLA UV printer [25]. PEEK is another potential alternative thermoplastic as it is lower loss than ABS [22]. PEEK is more durable as well making it a more likely choice in a high stress environment [2]. However, it is a challenging material to print with and due to scope and time constraints it was not

implemented in this design but would be an interesting future consideration to get better insertion loss.

A more defined method for matching the feed can be studied. The thickness and the width of the slot determine the impedance matching of the circuit and the correct solution was achieved empirically. The impedance calculations for the slot showed to be different from the ones for a traditional slot and from the Knor balun or the impedance of the slot line section is greatly changed by the addition of the coupling structure.

The MSM structure can be further validated in a full network such as a printed conformal antenna being fed completely wirelessly. Based on the measurements and simulation shown in this thesis it possible to integrate the MSM well into a conformal antenna design.

References

[1] D. Bell and Fallat, "The Future of Additive Manufacturing in the US Military," in "Mfg & Industrial Eng & Control of Product Sys," 2017. [Online]. Available: https://apps.dtic.mil/dtic/tr/fulltext/u2/1042079.pdf

[2] C. Neff, E. Elston, M. Burfeindt, N. Crane, and A. Schrand, "A fundamental study of printed ink resiliency for harsh mechanical and thermal environmental applications," Additive Manufacturing, vol. 20, pp. 156-163, 2018/03/01/ 2018, doi: https://doi.org/10.1016/j.addma.2018.01.009.

[3] G. Kumar and K. P. Ray, “Chapter 4: Multilayer broad band MSAs,” in Broadband microstrip antennas, Boston, MA: Artech House, 2003.

[4] “RF Wireless World,” Slotline basics | Slotline types. [Online]. Available: https://www.rfwireless-world.com/Articles/Slotline-basics-and-slotline-types.html. [Accessed: 05-Nov-2022].

[5] F. T. Ulaby and U. Ravaioli, “Fundamentals of Applied Electromagnetics”, 7th ed., Upper Saddle River, NJ: Pearson Education Limited, 2015, pp. 1–100.

[6] J. B. Knorr, "Slot-Line Transitions (Short Papers)," in IEEE Transactions on Microwave Theory and Techniques, vol. 22, no. 5, pp. 548-554, May 1974, doi: 10.1109/TMTT.1974.1128278.

[7] P. Mondal, A. Roy, and S. K. Parui, “Wide-band Bandpass filter using CRLH transmission line and floating slot approach,” Procedia Technology, vol. 4, pp. 466–471, 2012.

[8] E. A. Rojas-Nastrucci, Ramiro Ramirez and T. M. Weller, "Direct Digital Manufacturing of mm-Wave Vertical Interconnects," 2018 IEEE 19th Annual Wireless and Microwave Technology Conference (WAMICON), April 2018.

[9] S. LeBlanc, K. Church, E. A. Rojas-Nastrucci, E. Martinez-de-Rioja, E. Carrasco, and J. A. Encinar, "Advanced Manufacturing and Characterization of mm-Wave Two-Layer Reflectarray Cells," 2022 IEEE 22nd Annual Wireless and Microwave Technology Conference (WAMICON), 2022, pp. 1-4, doi: 10.1109/WAMICON53991.2022.9786075.

[10] C. R. Mejias-Morillo et al., "High-Temperature Additively Manufactured C-Band Antennas Using Material Jetting of Zirconia and Micro-Dispending of Platinum Paste," in IEEE Open Journal of Antennas and Propagation, vol. 3, pp. 1289-1301, 2022, doi: 10.1109/OJAP.2022.3218798.

[11] Thomas P. Ketterl, Yaniel Vega, Nicholas C. Arnal, John W. I. Stratton, Eduardo A. Rojas-Nastrucci, María F. Córdoba-Erazo, Mohamed M. Abdin, Casey W. Perkowski, Paul I. Deffenbaugh, Kenneth H. Church, and Thomas M. Weller, "A 2.45 GHz Phased Array Antenna Unit Cell Fabricated Using 3-D Multi-Layer Direct Digital Manufacturing," in IEEE Transactions on Microwave Theory and Techniques, vol. 63, no. 12, pp. 4382-4394, Dec. 2015.

[12] E. A. Rojas-Nastrucci, Harvey Tsang, Paul Deffenabugh, T. M. Weller, Ramiro A. Ramirez, D. Hawatmeh, and Kenneth Church, “Characterization and Modeling of K-Band Coplanar Waveguide Digitally Manufactured using Pulsed Picosecond Laser Machining of Thick-Film Conductive Paste,” in IEEE Transactions on Microwave Theory and Techniques, vol. 65, no. 9, pp. 3180-3187, Sept. 2017.

[13] Seng Loong Yu, Eduardo A. Rojas-Nastrucci, " Characterization of Microdispensed Dielectric Materials for Direct Digital Manufacturing Using Coplanar Waveguides," 2019 IEEE 20th Annual Wireless and Microwave Technology Conference (WAMICON), April 2019.

[14] Carlos R. Mejias-Morillo, and Eduardo A. Rojas-Nastrucci, “Z-Meandering Miniaturized Patch Antenna Using Additive Manufacturing,” 2020 IEEE Radio and Wireless Symposium (RWS), San Antonio, TX, 2020.

[15] R. A. Ramirez, E. A. Rojas-Nastrucci and T. M. Weller, "UHF RFID Tags for On-/Off-Metal Applications Fabricated Using Additive Manufacturing," in IEEE Antennas and Wireless Propagation Letters, vol. 16, pp. 1635-1638, 2017.

[16] R. Garg, I. J. Bahl, and M. Bozzi, “Slotlines,” in Microstrip lines and Slotlines, Boston: Artech House, 2013.

[17] J. J. Lee, "Slotline impedance," in IEEE Transactions on Microwave Theory and Techniques, vol. 39, no. 4, pp. 666-672, April 1991, doi: 10.1109/22.76430.

[18] R. Janaswamy and D. H. Schaubert, “Characteristic impedance of a wide slotline on low-permittivity substrates (short paper),” IEEE Transactions on Microwave Theory and Techniques, vol. 34, no. 8, pp. 900–902, 1986.

[19] F. Castles et al, "Microwave dielectric characterization of 3D-printed BaTiO3/ABS polymer composites," Scientific Reports (Nature Publisher Group), vol. 6, pp. 22714, 2016. Available: http://ezproxy.libproxy.db.erau.edu/login?url=https://www.proquest.com/scholarly-journals/microwave-dielectric-characterisation-3d-printed/docview/1898715358/se-2. DOI: https://doi.org/10.1038/srep22714.

[20] M. Pérez-Escribano and E. Márquez-Segura, "Parameters Characterization of Dielectric Materials Samples in Microwave and Millimeter-Wave Bands," in IEEE Transactions on Microwave Theory and Techniques, vol. 69, no. 3, pp. 1723-1732, March 2021, doi: 10.1109/TMTT.2020.3045211.

[21] Deffenbaugh, Paul I., "3D Printed Electromagnetic Transmission and Electronic Structures Fabricated on A Single Platform Using Advanced Process Integration Techniques" (2014). Open Access Theses & Dissertations. 1228. https://digitalcommons.utep.edu/open_etd/1228

[22] K. B. R. F. Cafe, “Dielectric constant, strength, & loss tangent,” Dielectric Constant, Strength, & Loss Tangent - RF Cafe. [Online]. Available: https://www.rfcafe.com/references/electrical/dielectric-constants-strengths.htm. [Accessed: 11-Feb-2022].

[23] Rogers Corporation, RO4000 Series High Frequency Circuit Materials. Rogers Corporation, Chandler, AZ, 2022.

[24] F. Giannini, R. Sorrentino and J. Vrba, "Planar Circuit Analysis of Microstrip Radial Stub (Short Paper)," in IEEE Transactions on Microwave Theory and Techniques, vol. 32, no. 12, pp. 1652-1655, Dec. 1984, doi: 10.1109/TMTT.1984.1132907.

[25] Rogers Corporation, Radix Printable Dielectric. Rogers Corporation, Chandler, AZ, 2022.